Wave rafting and the equilibrium pancake ice cover thickness

Mingrui Dai and Hayley H. Shen
Department of Civil and Environmental Engineering, Clarkson University, Potsdam, New York, USA

Mark A. Hopkins
Cold Regions Research and Engineering Laboratory, Hanover, New Hampshire, USA

Stephen F. Ackley
Department of Civil and Environmental Engineering, Clarkson University, Potsdam, New York, USA

Received 3 November 2003; revised 20 February 2004; accepted 15 April 2004; published 31 July 2004.

[1] Pancake ice, the circular floes formed during ice growth in a wave field, forms in many polar and subpolar seas. Vertical thin sections of cores taken from the ice cover in these regions show distinct layering structure. These observations suggest wave rafting could play a significant role in defining the ice cover thickness, much more so than thermodynamic growth. Although wave rafting is intuitively apparent, no previous study relating the resulting ice cover to wave characteristics has been conducted. In this study we utilize both laboratory experiments and numerical simulations to determine the rafting process. We propose a theory that predicts a final equilibrium thickness, provided that the incoming wave is kept constant. The equilibrium thickness from the theory is proportional to the square of the wave amplitude and the square of the floe diameter and is inversely proportional to the cube of the wavelength. This theory relates the final ice cover thickness to the wave characteristics and the size and surface properties of the pancake ice floes. This theory also provides a way to calculate the speed with which the boundary between the single-layer pancake ice floes and the equilibrium rafted ice cover propagates. We conduct laboratory experiments with plastic model pancake ice to create rafting. We perform computer simulations with a three-dimensional discrete element model that simulates the movement of disc-shaped floes in the wave field. We compare the theoretical result with the laboratory experiments and a numerically simulated rafting process. Both the laboratory and the computer simulation results compare favorably with the theory. *INDEX TERMS:* 4540 Oceanography: Physical: Ice mechanics and air/sea/ice exchange processes; 4560 Oceanography: Physical: Surface waves and tides (1255); 4572 Oceanography: Physical: Upper ocean processes; 4207 Oceanography: General: Arctic and Antarctic oceanography; 4294 Oceanography: General: Instruments and techniques; *KEYWORDS:* pancake ice, wave rafting, equilibrium ice thickness, ice-wave interaction, polar oceanography

Citation: Dai, M., H. H. Shen, M. A. Hopkins, and S. F. Ackley (2004), Wave rafting and the equilibrium pancake ice cover thickness, *J. Geophys. Res.*, *109*, C07023, doi:10.1029/2003JC002192.

1. Introduction

[2] Sea ice forms at the interface between the ocean and the atmosphere, two major components of the global climate system. Sea ice reflects more short-wave radiation than the open ocean, affects the amount of heat and moisture that is exchanged between ocean and atmosphere, and thus plays an important role in the global climate change. Ice can also affect the global climate in another way. At high latitudes, salinity is the main factor that determines seawater density. When ice forms on the sea surface, the rejected salt increases the water density just below the ice cover. This cold and dense water sinks and is believed to be one of the driving forces of deep ocean circulation. To replace the sinking water, warm water from low latitude moves to high latitude and drastically changes the high-latitude water temperature. Without this warm water the temperature in high latitude would be much colder. The upwelling to the surface of lower-latitude water also serves to ventilate the ocean water by contact with the atmosphere, which primarily occurs at high latitudes [*Siedler et al.*, 2001].

[3] The first stage in sea ice development is the formation of individual ice crystals in the surface layer of the ocean. These crystals, known as frazil ice, form in open water areas when the temperature of the water is below freezing. With further freezing, the crystals coagulate to form a layer known as grease ice. How the sea ice proceeds from this point on depends on whether the surface is calm or disturbed. With calm conditions the frazil and grease ice

Copyright 2004 by the American Geophysical Union.
0148-0227/04/2003JC002192

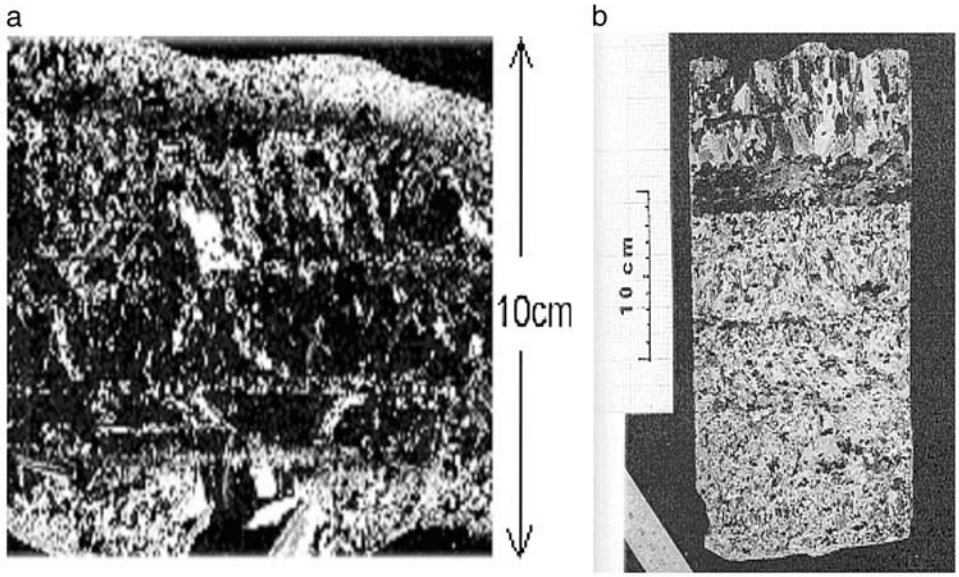

Figure 1. Vertical thin section of a pancake ice cover. (a) Floe from the Weddell Sea that consists of three layers of individual pancakes rafted together [*Ackley and Shen*, 1996]. (b) Floe from the Sea of Okhotsk having five layers [*Toyota*, 1998].

may consolidate into continuous flexible sheets called nilas. Under rough conditions, with the influence of waves the frazil crystals coagulate and consolidate into small circular discs called pancake ice. The pancakes have raised rims formed by collisions with other pancakes. They also grow by accumulating ice crystals from the surrounding water and from bonding with neighboring discs. The size of the pancakes may rapidly increase to a few meters in diameter and up to 0.4 m thick. As the penetrating waves gradually lose energy, the pancakes freeze together to form a consolidated ice cover. This process of ice formation is responsible for a significant percentage of sea ice production in the Southern Ocean [*Wadhams*, 1991; *Meldrum et al.*, 2000].

[4] Although rafting is intuitively apparent, direct field observation is difficult to make. The timing of cruises to make appropriate wave and ice measurements to coincide with rapid ice cover growth and expansion (over hours to a day or two) is prohibitively challenging. However, indirect observations made after the wave-ice interaction episode have revealed clear evidence of the rafting process. In Figure 1 the ice core samples taken in the Weddell Sea [*Ackley and Shen*, 1996] and the Sea of Okhotsk [*Toyota*, 1998] show layered structures in the thin section. Typically, the number of layers varied from two up to seven. In addition to rafting, *Doble et al.* [2003] presented a top layer freezing mechanism for the generation of layered pancakes.

[5] A better understanding of the mechanical thickening on top of thermodynamic thickening of a pancake ice field is critical to a more accurate formulation of spatial and temporal change of ice thickness. Here mechanical thickening is defined as the redistribution of existing ice volume, and thermodynamic thickening is the increase of ice volume due to heat loss. *Martin and Kauffman* [1981] and *Bauer and Martin* [1983] studied frazil ice cover thickening. They presented both laboratory data and theoretical arguments relating frazil ice cover thickness to wave/wind parameters. Their findings suggested that the ice growth rate in a wave field is an order of magnitude greater than the one-dimensional thermal growth model [*Anderson*, 1961]. *Hibler and Ackley* [1983] showed that thermodynamic ice models, even corrected with additional ice internal stress, greatly underestimated the Weddell Sea ice area evolution in the formation season. The dynamics near the ice edge are extremely sensitive to thickness. If wave rafting effectively increases the thickness at the expense of areal growth at the ice boundary, new ice at the edge could survive diurnal air temperature oscillations to accelerate seasonal ice cover growth. In a comparison of sea ice dynamics models, *Hunke and Zhang* [1999] found that the difference in the ice concentration and thickness distribution between two ice models appears mainly at the ice boundary. Sensitivity of sea ice models has been demonstrated to amplify near the ice boundary [*Hibler and Ackley*, 1983; *Geiger et al.*, 1997]. Currently, no air-ice-ocean models include wave effects. Apparently, waves may increase the surface turbulence and hence the heat loss rate. But more importantly, waves advect ice floes to create new open water for more ice production. Waves also raft ice floes together to rapidly thicken the ice cover, thus effectively increasing the in situ ice growth.

[6] *Bauer and Martin* [1983] studied the growth and pileup of frazil ice in small leads. The driving force in their model is the wave radiation stress and wind-induced current. The resisting force is the hydrodynamic pressure gradient generated from the slope of the free surface. In this study we will present a model to explain the pancake ice cover thickening process in an open ocean. We can idealize the situation of mechanical thickening of a pancake ice field as shown in Figure 2. Pancake ice floes are driven by waves toward the pack ice and pile up in front of it. The pileup is frozen to become part of the pack ice. The thickness of the pileup becomes the initial thickness of the new pack ice. It is of interest to investigate the horizontal ice thickness distribution and the progression velocity of the ice boundary defined as the boundary between the pack ice

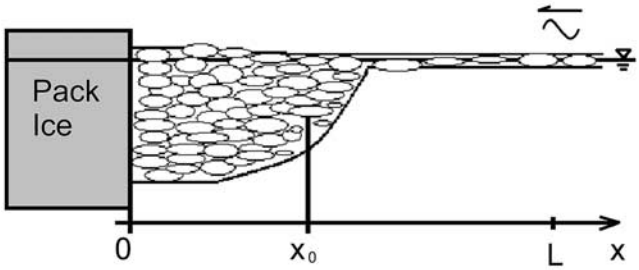

Figure 2. Definition sketch of ice thickness distribution.

and the compacting pancake ice. In studying the movement of pancake ice in a wave field, *Hopkins and Shen* [1998] suggested the existence of an equilibrium thickness in front of pack ice on the basis of numerical experiment results. In their study, they utilized a three-dimensional discrete element model to simulate the movement of pancake ice in a wave field. A nonreflecting barrier, placed at the end of the calculation domain, simulated pack ice. They found that the force acting on the barrier leveled off after a long period of steady increase, suggesting the existence of an equilibrium thickness. *Shen and Zhong* [2001] studied the drift of a single small floe under wave action with and without wave reflection and provided theoretical solutions for simple cases. The drift velocity of a group of ice floes was studied by *Frankenstein and Shen* [1993].

[7] In this study, we try to answer three fundamental questions: (1) Given ice characteristics and wave parameters, is there an equilibrium thickness? If yes, (2) what is the equilibrium thickness? (3) What is the progression velocity of this equilibrium thickness? We begin with a theoretical analysis based on principles of mechanics. We then compare the theoretical result with laboratory experiments and computer simulations.

2. Theoretical Analysis

[8] We envision a typical horizontal distribution of the rafted ice thickness as shown in Figure 2. Waves travel in the direction from open water to the pack ice and drive the ice floes toward the pack ice. L is the length of our domain of interest and x_0 is the position where the equilibrium rafted ice meets the compacting pancakes. Since this transition is gradual, we nominally define the location as halfway up the sloping profile, joining the pack ice boundary and the compacting pancakes. At the open ocean boundary, rafting is not present, and there is only one layer of ice. Each ice floe is subject to a water drag force, collision forces between ice floes, buoyancy, and gravity. These forces control the drift of pancake floes. Pancake floes stop drifting in front of the pack ice. Thereafter, the ice areal concentration increases first. If there is no wave action, the stopped ice floes will juxtapose with nearly 100% areal concentration, and that is the final stage. However, if there are waves, and if the wave amplitude is sufficient to jostle the floes out of their horizontal alignment, then rafting can occur. In this way, waves act as the compacting agent that thickens the pancake ice cover.

[9] Thickening of an ice cover composed of individual pieces has been thoroughly discussed by *Hopkins et al.* [1991] and *Hopkins and Tuhkuri* [1999]. *Hopkins et al.* [1991] used a failure criterion determined by the internal friction angle and the Mohr-Coulomb law to explain the final equilibrium thickness of the ridging process. *Hopkins and Tuhkuri* [1999] found that the Mohr-Coulomb condition was applicable to ridges as thin as $2 \sim 3$ floes. In the rafting case the postequilibrium aggregate of ice floes approximates a quasi-static state, so the Mohr-Coulomb law also governs the thickening process in wave-induced pancake rafting.

[10] To theoretically study the thickening process, we consider the floes as a granular material. When compacting granular materials, the internal friction created by the interparticle friction as well as the geometry of the packing resists compaction. When the stress state inside the granular assembly exceeds the yield strength on the basis of the Mohr-Coulomb criterion, the assembly fails. This situation is best explained by considering retention walls. When one pushes a vertical wall against a pile of soil, the soil fails and thickens behind the wall. In soil mechanics this phenomenon is called the passive state of failure (when withdrawing the wall, collapsing of the soil is the active state). The failure criterion for this passive state is described by

$$\sigma_x = [(1 + \sin\phi)/(1 - \sin\phi)]\sigma_z, \tag{1}$$

where σ_x is the normal stress exerted by the wall, σ_z is the normal stress due to gravity, and ϕ is the internal friction angle which is a function of both the interparticle friction and the packing geometry of the assembly [*Lambe and Whitman*, 1979].

[11] In the case of pancake ice in a wave field the active pushing comes from the waves. Floe collisions induced by the waves generate normal stresses within the granular assembly of floes. However, the packing geometry and the surface friction between floes resist this compaction/thickening. An effective internal friction angle for pancake ice piles exists. Given that a pile of floes acts the same as a soil pile, when the wave-induced normal stress exceeds the Mohr-Coulomb criterion as described in equation (1), we must have pile thickening. At the time when the normal stress becomes lower than the strength of the pile, equilibrium thickness is reached.

[12] Figure 3 shows a cross section of the pancake pile. We will use it to guide our thoughts on formulating the normal force induced by waves.

[13] The normal stress over the vertical cross section in the pileup is generated by impacts between particles.

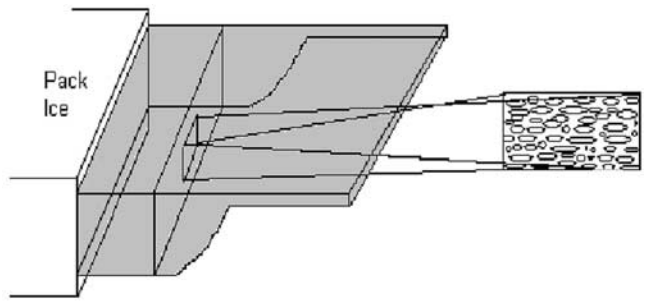

Figure 3. Cross section of a vertical layer in the pancake ice pileup.

Impact-induced stresses in a granular medium have been extensively studied in the past couple of decades [*Campbell*, 1990]. We follow the conceptual development first introduced by *Bagnold* [1954]. The impact force in a unit vertical area is proportional to the number of particles in this area, the frequency of impact, and momentum exchanged between particles during impact. That is,

$$\sigma_x = Nf\Delta M_x, \tag{2}$$

where σ_x is the x direction normal stress, N is the number of ice floes in unit vertical area, f is the collision frequency, and ΔM_x is the momentum change of each particle due to the impact.

[14] The number of ice floes may be estimated as $N \propto C/Dd$, where C is the vertical concentration, D is the diameter of a floe, and d is the thickness of a floe. The collision frequency f is estimated as the relative velocity between two floes divided by the distance between two floes. That is, $f = \Delta V/\Delta x$, where ΔV is the mean relative velocity between two floes and Δx is the mean distance between two floes. The mean relative velocity ΔV is proportional to the gradient of the local water velocity, $\Delta V \propto (\partial U/\partial x)\Delta x$, where U is the water velocity. Hence $f \propto (\partial U/\partial x) \propto \omega A e^{kz} k$, where ω is the angular frequency of wave, A is the wave amplitude, z is the vertical location, and k is the wave number.

[15] The exchange of momentum at each collision between floes is modeled as $\Delta M_x = m(\partial U/\partial x)\Delta x \propto \rho_i D^3 d\omega A e^{kz} k$, where m is the mass of one floe and ρ_i is the ice density. Here Δx is considered as the distance between the centers of two ice floes when collision happens. Because collisions can happen in a variety of pair configurations, this distance is approximately of order D.

[16] Substituting the expression for the number of ice floes, collision frequency, and momentum change into equation (2), we obtain the x direction normal stress as

$$\sigma_x \propto C\omega^2 A^2 k^2 \rho_i D^2 = K_c C\omega^2 A^2 e^{2kz} k^2 \rho_i D^2. \tag{3}$$

This stress compresses the pancake ice floes. When the pancake ice layer is thin, the normal stress in the z direction is small, and the failure criterion described by the Mohr-Coulomb condition equation (1) indicates that thickening must occur.

[17] As the ice cover rafts and thickens, the normal stress in the z direction increases. Referring to Figure 4, the normal stress in the z direction in the layer above the water level at an arbitrary location is

$$\sigma_z = (1-n)\rho_i g(h_1 - z), \tag{4}$$

where n is the porosity of ice, h_1 is the thickness of the layer above the water, and z is the vertical coordinate with origin at calm water. The normal stress in the z direction below the water at an arbitrary location is

$$\sigma_z = (1-n)\rho_i g(\rho_w/\rho_i - 1)(z + h_2), \tag{5}$$

where ρ_w is the density of water and h_2 is the total thickness below the water.

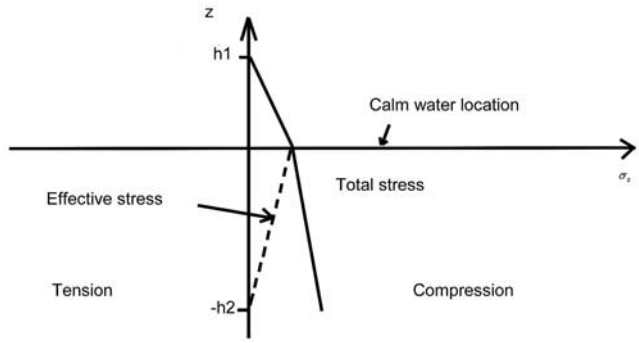

Figure 4. Vertical stress distribution.

[18] Since the pancake ice layer is free floating, we may assume a neutrally buoyant condition. Thus h_1 and h_2 are related to the overall thickness h by

$$h_1 = (1 - \rho_i/\rho_w)h \tag{6}$$

$$h_2 = (\rho_i/\rho_w)h. \tag{7}$$

[19] The average vertical normal stress can be obtained by integrating equations (4) and (5) over the thickness of the ice water layer using equations (6) and (7),

$$\overline{\sigma}_z = \frac{1}{h}\int_{-h_2}^{h_1} \sigma_z dz = \frac{1}{h}\left(\int_0^{h_1} \sigma_z dz + \int_{-h_2}^{0} \sigma_{z_x} dz\right) = Kh, \tag{8}$$

where $K = 1/2(1 - n)\rho_i g[1 - (\rho_i/\rho_w)]$ is a constant. As long as the rafting/thickening is underway, the average normal stress in the x direction is related to the z direction through equation (1). Therefore the total normal force resisting thickening for a pancake ice cover of thickness h is

$$F_r = \overline{\sigma}_x h = K_r h^2, \tag{9}$$

where

$$K_r = K\left(\frac{1+\sin\phi}{1-\sin\phi}\right) = \frac{1}{2}\left(\frac{1+\sin\phi}{1-\sin\phi}\right)(1-n)\rho_i g\left(1 - \frac{\rho_i}{\rho_w}\right). \tag{10}$$

As the thickening progresses, the resistance force increases and eventually, when the resisting force equals the compacting force, equilibrium thickness is reached.

[20] Integrating equation (3) in the range of ice thickness and assuming that the wave is a simple wave gives

$$F = \frac{K_c C g A^2 k^2 \rho_i D^2}{2}\left(1 - e^{-2kh}\right). \tag{11}$$

Expanding e^{-2kh} and neglecting terms of 3rd order or higher, we have

$$\begin{aligned} F &= \frac{K_c C g A^2 k^2 \rho_i D^2}{2}\left[1 - \left(1 - 2kh + 2k^2h^2\right)\right] \\ &= K_c C g A^2 k^3 \rho_i D^2 h(1 - kh). \end{aligned} \tag{12}$$

Figure 5. Wave tank.

Equating equation (3) with equation (12), we have

$$h = \frac{K_c C \omega^2 A^2 k^2 \rho_i D^2}{K_r - K_c C \omega^2 A^2 k^2 \rho_i D^2}. \quad (13)$$

Equation (13) provides a way to estimate the equilibrium pancake ice cover thickness under wave rafting.

[21] For most parts of the ocean where pancake ice forms, the depth of water is much greater than a typical wavelength, and a deep water dispersion relation $\omega^2 = gk$ is assumed. This assumption may be removed without affecting the theory we will develop below.

[22] Assuming that rafting occurs at maximum areal concentration where $C = 1$, equation (13) can be rewritten as

$$h = \frac{K_c g A^2 k^3 \rho_i D^2}{K_r - K_c g A^2 k^3 \rho_i D^2}. \quad (14)$$

We define $S = Ak$ as dimensionless wave steepness, $D' = kD$ as dimensionless ice floe diameter, $K_r' = 1/2[(1 + \sin \phi)/(1 - \sin \phi)](1 - n)[1 - (\rho_i/\rho_w)]$ as the dimensionless friction coefficient, and $h' = hk$ as dimensionless thickness. Equation (14) can be expressed in terms of these dimensionless variables as

$$h' = \frac{K_c S^2 D'^2}{K_r' - K_c S^2 D'^2}. \quad (15)$$

For field scale, S and D' are small values compared with K_r'; therefore equation (15) can be further simplified as

$$h' = \frac{K_c}{K_r'} S^2 D'^2 \quad (16a)$$

or

$$h = (2\pi)^3 \frac{K_c}{K_r'} \frac{A^2 D^2}{\lambda^3}, \quad (16b)$$

where $\lambda = 2\pi/k$ is the wavelength.

[23] After the wave rafting produces an equilibrium thickness in front of the pack ice, further incoming single-layer pancake floes continue the rafting process and cause the ice boundary to progress. The thickening profile propagates toward the incoming wave. Referring to Figure 2, this ice boundary is defined as the middle point of the sloping ice thickness transition section. Assuming that the ice thickness profile may be approximated by a linear profile, from mass conservation we have

$$LC_0 d + VdC_0 t = (L - x_0)C_0 d + x_0 h, \quad (17)$$

where L is the length of calculation domain, C_0 is the ice concentration at position L, d is the thickness of one ice floe, V is the drift velocity of the ice floe, x_0 is the position of the ice boundary, and h is the equilibrium thickness of the rafted ice. The concentration in the rafted region is assumed to be 1.

[24] Solving x_0 from equation (17), we have the position of ice boundary varying with time,

$$x_0 = VdC_0 t/(h - C_0 d). \quad (18)$$

The progression velocity of the ice boundary is therefore

$$\frac{dx_0}{dt} = VdC_0/(h - C_0 d). \quad (19)$$

Thus the propagation of the boundary of the rafted pancake ice has a speed proportional to the free drift of the ice induced by the wave field, which agrees with intuition.

3. Experimental Verification

[25] Both physical and numerical experiments are carried out to verify the proposed theory. In the following sections, we will first introduce the physical experiments.

3.1. Wave Tank Experiment

[26] A series of experiments were carried out in the wave tank of Clarkson University's Civil and Environmental Engineering Department. The wave tank is 18 m in length and 1.8 m in width. At one end a single-stroke flap-type wave maker was installed to generate waves. At the other end a stainless steel beach having a circular profile was set up to dissipate the wave energy. A comb-shaped barrier was installed to simulate the pack ice while letting the wave pass through with negligible reflection, as shown in Figure 5. A pressure transducer array of eight sensors was used to estimate the wave height and wave number. A video camera was used to film the movement of the square floes. The layout of the wave tanks and the location of the instruments are shown in Figure 6.

[27] The ice blocks were cut from a plastic sheet. The dimensions are $0.05 \times 0.05 \times 0.006$ m. The Young's modulus is $(1.8 \pm 0.2) \times 10^9$ Pa [*Frankenstein*, 1996]. The transducer is model PX439 005GI, manufactured by

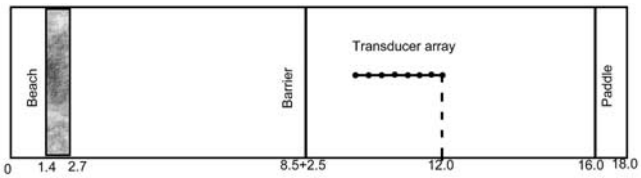

Figure 6. Layout of the instruments.

Table 1. Parameters of the Wave Tank Experiments

Experiment	Water Depth, m	Transducer Depth, m	Frequency, Hz	Paddle Stroke Setting		
				Maximum	Middle	Low
3	51.5	17.5	0.78	X		
4	51.5	17.5	0.82	X		
1	56.0	22.0	0.86	X		
5	51.5	17.5	0.86	X		
2	51.5	17.5	0.90		X	
8	51.5	33.5	0.90		X	
6	51.5	17.5	1.02		X	
7	51.5	17.5	1.13			X

Omega Engineering Inc. The first transducer was located at 12 m, and the interval between transducers varied from 0.2 to 0.25 m according to the wave frequency. The total length between the first and the last transducer was less than 1 wavelength. For most cases the depth of the transducer was 0.17 m below the calm water surface. When water depth was 0.56 m, the transducer depth was 0.22 m. In one case the transducer was 0.335 m below the calm water level. The data collection and processing procedures are described by *Evers et al.* [2002] and *Shen et al.* [2002].

[28] The thickness of the ice layer was determined visually when the pileup was less than five layers. When the thickness was large, the ice layer was filmed by video camera on a side window. The thickness was estimated using the images captured from the video recording. A combination of water depth, frequency, and paddle stroke was used to generate waves of different wave height and wave number. The settings of the experiment are summarized in Table 1.

3.2. Numerical Experiment

[29] Because of the difficulties of collecting field data, a three-dimensional discrete element model [*Hopkins and Tuhkuri*, 1999; *Hopkins and Shen*, 1998] is used to carry out a series of numerical experiments to simulate the ice-wave interactions at field scale. The data collected from these experiments are used to check against the theory developed in section 2. The model ice floes are circular discs with a circular edge. The floe aspect ratio is variable. This model explicitly simulates the behavior of each ice floe. For details of the model, readers are referred to *Hopkins and Tuhkuri* [1999]. The parameters used in the experiments are summarized in Tables 2 and 3. Parameters common to all experiments are summarized in Table 4. In Tables 2 and 3 the friction coefficient is that between floes, not the internal friction of the floe assembly. For frictionless cases the friction coefficient between floes is 0. The thickness of the ice layer is defined as the distance between the surface of the topmost ice floe and the bottom of the bottommost ice floe at a randomly picked location. It took more than 4 months to run the total 27 cases on two P4 1.4 GHz computers. Each of the 27 cases required roughly 6000 floes to reach the equilibrium stage.

4. Results

4.1. Wave Tank Experiment

[30] In this section we will summarize the results of the experiments. To verify the theoretical relationship between dimensionless equilibrium rafted ice thickness h' and the parameter S^*D', we applied regression analysis to the experimental data to see if there is a significant relationship between them. Taking the logarithm of both sides of equation (16a),

$$\log(h') = \log\left(\frac{K_c}{K_r'}\right) + 2^* \log(S^*D'). \tag{20}$$

We applied linear regression analysis to the observed $\log(h')$ and $\log(S^*D')$ and present the results in Figure 7. The t test was made using the statistical package Origin (OriginLab® Corporation).

Table 2. Parameters of Numerical Experiments for Frictionless Cases

Experiment	Wave Height, m	Wavelength, m	Wave Frequency, Hz	Calculation Duration, s	Friction Coefficient μ
12	3.0	60	0.1613	8000	0
13	1.0	80	0.1397	8000	0
14	2.5	80	0.1397	8000	0
15	3.0	80	0.1397	8000	0
16	3.5	80	0.1397	8000	0
17	4.0	80	0.1397	8000	0
18	4.5	80	0.1397	8000	0
19	5.0	80	0.1397	4800	0
20	1.0	100	0.1250	12000	0
21	2.5	100	0.1250	12000	0
22	3.0	100	0.1250	8000	0
23	3.5	100	0.1250	8000	0
24	4.0	100	0.1250	8000	0
25	4.5	100	0.1250	8000	0
26	5.0	100	0.1250	8000	0
27	4.0	120	0.1141	8000	0

Table 3. Parameters of Numerical Experiments for Frictional Cases

Experiment	Wave Height, m	Wavelength, m	Wave Frequency, Hz	Calculation Duration, s	Friction Coefficient μ
1	2.5	80	0.1397	8000	0.35
2	3.5	80	0.1397	8000	0.35
3	2.5	100	0.1250	8000	0.35
4	3.0	100	0.1250	8000	0.35
5	3.5	100	0.1250	8000	0.35
6	4.0	100	0.1250	8000	0.35
7	4.5	100	0.1250	8000	0.35
8	3.0	120	0.1141	8000	0.35
9	3.5	120	0.1141	8000	0.35
10	4.0	120	0.1141	8000	0.35
11	4.5	120	0.1141	8000	0.35

[31] Figure 7 shows the relationship between observed dimensionless equilibrium rafted ice thickness h' and the parameter S^*D'. The slope of the best fit curve is 2.07, which agrees with the theoretical value of 2. The 95% confidence level range for the slope is (1.2, 2.94). The intercept of the fitted line is −2.12, and the 95% confidence level range for the intercept is (−2.55, −1.69). The F statistic is 33.76, greater than the F distribution value $F(1, 6, 0.99) = 16.26$ [*Draper and Smith*, 1981]. Hence the regression passes the 99% confidence level test. In other words, we establish that the relationship exists between $\log(h')$ and $\log(S^*D')$, running a risk of less than 1% chance of error.

4.2. Numerical Experiment

[32] The results of the numerical experiment are summarized in Tables 5 and 6. To determine the equilibrium ice cover thickness, we calculate the ice layer thickness at 5000 locations evenly distributed along the central line of the calculation domain. The thickness profile is then smoothed by a running average. The ice layer thickness at a given location is defined as the distance between the surface of the topmost ice floe and the bottom of the bottommost ice floe. An example of the numerically simulated ice rafting is shown in Figure 8.

[33] The relations between dimensionless ice thickness and the product of dimensionless wave steepness and dimensionless floe diameter are analyzed and are presented in Figures 9 and 10. From Figures 9 and 10 we can see that the slopes of the fitted curve are close to 2, the theoretical value. The 95% confidence level range of the slope for the frictionless case is (1.46, 2.04). For the frictional case it is (1.6, 2.07). The best fit intercepts are 2.64 for the frictionless and 3.42 for the frictional case. The 95% confidence level ranges of the intercepts are (2.01, 3.26) for the frictionless case and (2.84, 4) for the frictional case. The regressions all passed the 99% confidence level under the F test. The frictionless case yielded F statistic value of 171, and the frictional case yielded 316. They are both greater than the required F distribution value of 9.07 for frictionless cases and 10.56 for frictional cases for the 99% confidence level.

Table 4. Common Parameters Used in the Model

Parameter	Value
Domain length, m	600
Domain width,[a] m	3.75
Floe diameter, m	1.0
Floe thickness, m	0.167
Ice density, kg/m^3	900
Water density, kg/m^3	1000
Normal contact stiffness, kN/m	167
Coefficient of restitution	0.25
Form drag coefficient	0.6
Viscous dumping coefficient	0.4

[a]With period boundary condition.

5. Discussion

[34] From the theoretical analysis presented in this study, we expect that pancake ice formed in a wave field will first drift. If stopped by the stationary pack ice, the pancake floes can raft under sufficient wave action. After the initial buildup period, rafted pancakes will reach an equilibrium thickness. This equilibrium thickness is proportional to the square of the wave amplitude and the square of the floe diameter and is inversely proportional to the cube of the wavelength. Thickness dependence on frictional properties of the floes is unclear, since both K_r' and K_c depend on friction. Comparing Figures 9 and 10, the equilibrium thickness for frictional cases is greater than the corresponding thickness for frictionless cases. Our

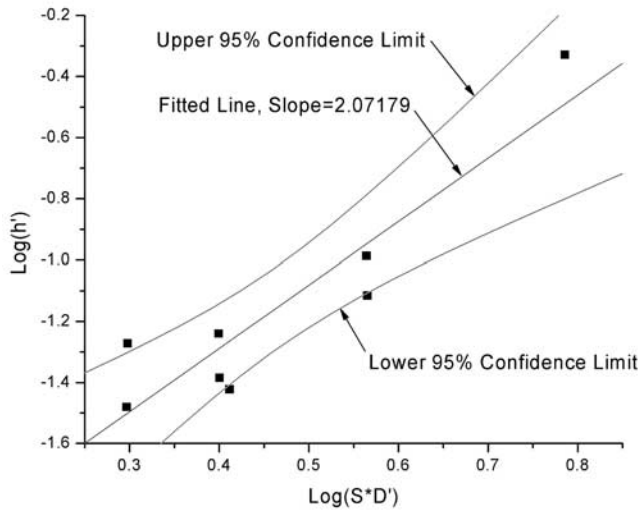

Figure 7. Result of the t test showing the relationship between dimensionless ice thickness h' and the product of dimensionless wave steepness and dimensionless floe diameter S^*D' from physical experiments.

Table 5. Numerical Experiment Results for Frictionless Cases

Wave Height, m	Wavelength, m	Wave Frequency, Hz	Ice Thickness, m
3.0	60	0.1613	3.8
1.0	80	0.1397	0.2
2.5	80	0.1397	0.8
3.0	80	0.1397	1.1
3.5	80	0.1397	1.8
4.0	80	0.1397	3.1
4.5	80	0.1397	4.7
5.0	80	0.1397	3.4
1.0	100	0.1250	0.2
2.5	100	0.1250	1.0
3.0	100	0.1250	0.7
3.5	100	0.1250	1.3
4.0	100	0.1250	1.1
4.5	100	0.1250	1.3
5.0	100	0.1250	2.8
4.0	120	0.1141	0.7

numerical data show for this parameter set that both K_r' and K_c increase with friction. Whether this is a general trend remains to be seen.

[35] The numerical experiments conducted indicate that equilibrium thickness is established in 2–3 hours for the field scale near the pack ice. Propagation of this equilibrium thickness is given in equation (19). The extent of the final ice cover depends on the duration of the rafting action. The equilibrium thickness is established even faster in the physical experiments at lab scale. Thus wave-induced rafting can produce ice cover thicknesses that are much larger than the thermodynamic growth alone.

[36] The dimensionless expression of the thickness $h' = (K_c/K_r')S^2D'^2$ covers both laboratory and field scales of interest. To apply this theory to real world problems, it is necessary to determine K_c/K_r', which is material property–dependent. Further work needs to be done before this theory can be put to practical use.

[37] There is some difference between the best fit slope of the numerical experiment result and that of the physical experiment result. The reason for this difference may be that the computer model neglects the interactions between water velocity potentials generated by the movement of individual particles. Another possible reason is that in the current implementation of the hydrodynamics, only the bottom layer of floes is exposed to the water drag force. Finally, the hydrodynamic interaction between water and floes is scale-dependent. The relative importance of each forcing term on floe dynamics may change from one scale to the other. As shown in the comparison of different friction coefficients, we suspect that the slope of the curve can be affected by all model parameters, including the hydrodynamic coefficients. A thorough parametric study will be carried out in due course. Future improvements may be necessary to fine tune the numerical model. However, the agreement we are able to obtain so far is encouraging.

Table 6. Numerical Experiment Results for Frictional Cases

Wave Height, m	Wavelength, m	Wave Frequency, Hz	Ice Thickness, m
2.5	80	0.1397	1.2
3.5	80	0.1397	2.6
2.5	100	0.1250	0.7
3.0	100	0.1250	1.1
3.5	100	0.1250	1.4
4.0	100	0.1250	1.6
4.5	100	0.1250	1.8
3.0	120	0.1141	0.6
3.5	120	0.1141	0.8
4.0	120	0.1141	1.1
4.5	120	0.1141	1.1

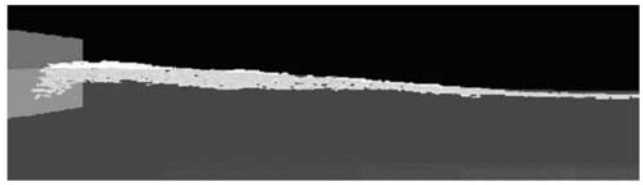

Figure 8. Ice floes in the simulation.

6. Conclusion

[38] A theoretical expression relating the equilibrium thickness of the buildup of rafted pancake ice floes in front of pack ice to the wave parameters and ice characteristics is proposed. The equilibrium ice thickness is proportional to the square of wave height and the square of the floe diameter and is inversely proportional to the cube of the wavelength. Friction between floes retards the rafting and produces smaller ice cover thickness. The propagation speed of the equilibrium thickness is proportional to the drift velocity of the floes and inversely proportional to the equilibrium cover thickness. The wave tank experiment results and numerical model results agree reasonably well with the theoretical prediction. The results presented here can have significant effect on how ice boundary dynamics are handled in current air-ice-ocean models. Implementation of this concept into large-scale numerical models is a necessary next step. This study shows that for air-ice-ocean coupled modeling, dynamics near the ice edge may be modified in such a way that total ice volume may be determined by existing frazil ice production models, but the thickness may be parameterized using the wave rafting

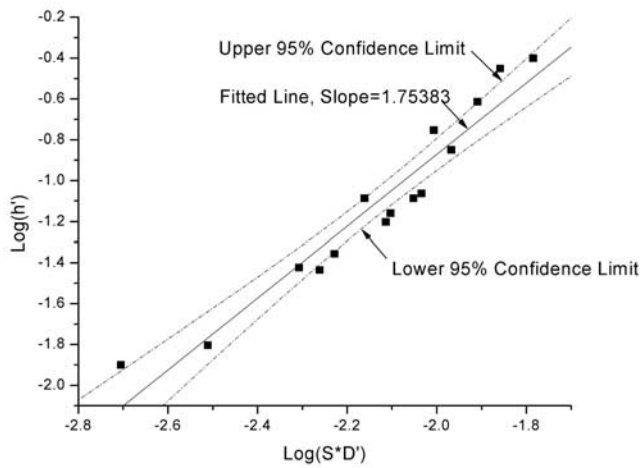

Figure 9. Relationship between dimensionless ice thickness h' and the product of dimensionless wave steepness and dimensionless floe diameter $S*D'$ for frictionless cases.

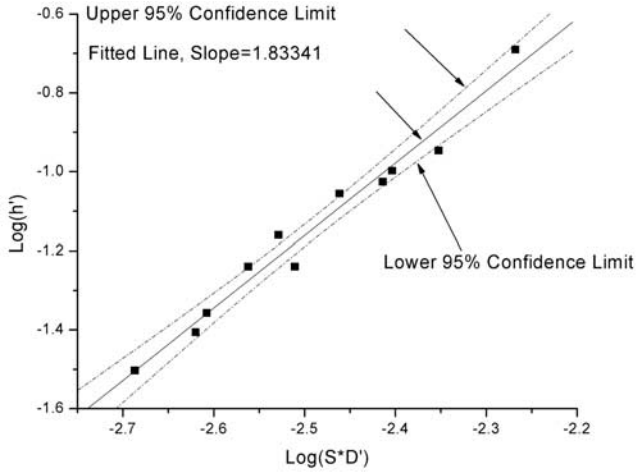

Figure 10. Relationship between dimensionless ice thickness h' and the product of dimensionless wave steepness and dimensionless floe diameter S^*D' for frictional cases.

results, and the areal coverage may be calculated as the volume divided by the thickness. It would be very interesting to test this new ice edge model to see if the current shortcomings in modeling ice edge progression mentioned in section 1 can be removed.

[39] **Acknowledgments.** This study was supported by the U. S. National Science Foundation Polar Program grant OPP-9814968. We would like to thank Dr. Takenobu Toyota for valuable discussions.

References

Ackley, S. F., and H. H. Shen (1996), Pancake ice formation in a laboratory wave tank, *Eos Trans. AGU*, *77*(22), West. Pac. Geophys. Meet. Suppl., 54.

Anderson, D. L. (1961), Growth rate of sea ice, *J. Glaciol.*, *3*, 1170–1172.

Bauer, J., and S. Martin (1983), A model of grease ice growth in small leads, *J. Geophys. Res.*, *88*, 2917–2925.

Bagnold, R. A. (1954), Experiments on a gravity-free dispersion of large solid spheres in a Newtonian fluid under shear, *Proc. R. Soc. London, Ser. A*, *225*, 49–63.

Campbell, C. S. (1990), Rapid granular flows, *Annu. Rev. Fluid Mech.*, *22*, 57–92.

Doble, M., M. D. Coon, and P. Wadhams (2003), Pancake ice formation in the Weddell Sea, *J. Geophys. Res.*, *108*(C7), 3209, doi:10.1029/2002JC001373.

Draper, N. R., and H. Smith (1981), *Applied Regression Analysis*, 2nd ed., John Wiley, Hoboken, N. J.

Evers, K.-U., H. H. Shen, M. Dai, Y. Yuan, T. Kolerski, and J. Wilkinson (2002), A twin wave tank pancake ice growth experiment, paper presented at 16th IAHR Ice Symposium, Int. Assoc. for Hydraul. Res., Dunedin, New Zealand, 12–16 Dec.

Frankenstein, S. (1996), The effects of waves on pancake ice, Ph.D. dissertation, 244 pp., Clarkson Univ., Potsdam, N. Y.

Frankenstein, S., and H. H. Shen (1993), The effect of waves on pancake ice collisions, *Proceedings of the Third International Offshore and Polar Engineering Conference*, edited by J. S. Chung, pp. 712–717, Int. Soc. of Offshore and Polar Eng., Cupertino, Calif.

Geiger, C. A., S. F. Ackley, and W. D. Hilber III (1997), Year-round pack ice in the Weddell Sea, Antarctica: Response and sensitivity to atmospheric and oceanic forcing, *Ann. Glaciol.*, *25*, 269–275.

Hibler, W. D., and S. F. Ackley (1983), Numerical simulation of Weddell Sea pack ice, *J. Geophys. Res.*, *88*, 2873–2887.

Hopkins, M. A., and H. H. Shen (1998), Simulation of pancake ice in a wave field, paper presented at 12th Engineering Mechanics Conference, Am. Soc. of Civil Eng., La Jolla, Calif., 17–20 May.

Hopkins, M. A., and J. Tuhkuri (1999), Compression of floating ice fields, *J. Geophys. Res.*, *104*, 15,815–15,825.

Hopkins, M. A., W. D. Hibler III, and G. M. Flato (1991), On the numerical simulation of the sea ice ridging process, *J. Geophys. Res.*, *96*, 4809–4820.

Hunke, E. C., and Y. Zhang (1999), A comparison of sea ice dynamics models at high resolution, *Mon. Weather Rev.*, *127*, 396–408.

Lambe, T. W., and R. V. Whitman (1979), *Soil Mechanics, SI Version*, John Wiley, pp. 97–116, Hoboken, N. J.

Martin, S., and P. Kauffman (1981), A field and laboratory study of wave damping by grease ice, *J. Glaciol.*, *27*, 283–314.

Meldrum, D., M. Doble, D. Mercer, O. Peppe, P. Wadhams, and J. Wilkinson (2000), A study of the winter Antarctic marginal ice zone using an innovative ice drifter, paper presented at Oceanology International 2000, Spearhead Exhib., Brighton, UK.

Shen, H. H., and Y. Zhong (2001), Theoretical study of drift of small rigid floating objects in wave fields, *J. Waterw. Port Coastal Ocean Eng.*, *127*(6), 343–351.

Shen, H. H., Y. Yuan, and M. Dai (2002), Data assemblage–pancake ice growth in a twin tank at HSVA, Nov. 21–28, 2001, *Rep. 02-03*, Civil and Environ. Eng. Dep., Clarkson Univ., Potsdam, N. Y.

Siedler, G., J. Gould, and J. Church (Eds.) (2001), *Ocean Circulation and Climate: Observing and Modelling the Global Ocean*, Academic, San Diego, Calif.

Toyota, T. (1998), A study on growth processes of sea ice in the southern region of the Okhotsk Sea, evaluated from heat budget and sea ice sample analysis, Ph.D. dissertation, Hokkaido Univ., Sapporo, Japan.

Wadhams, P. (1991), Atmosphere-ice-ocean interactions in the Antarctic, in *Antarctica and Global Climatic Change*, edited by C. Harris and B. Stonehouse, pp. 65–81, Belhaven, London.

S. F. Ackley, M. Dai, and H. H. Shen, Department of Civil and Environmental Engineering, Clarkson University, Potsdam, NY 13699-5710, USA. (sackley@pol.net; daim@clarkson.edu; hhshen@clarkson.edu)

M. A. Hopkins, USACE Engineer Research and Development Center, Cold Regions Research and Engineering Laboratory, 72 Lyme Road, Hanover, NH 03755-1290, USA. (mark.s.hopkins@erdc.usace.army.mil)